Introduction to QCD and Jet II

Bo-Wen Xiao

Pennsylvania State University
and Institute of Particle Physics, Central China Normal University

Jet Summer School
McGill June 2012

Outline

1. Collinear Factorization and DGLAP equation
   - Transverse Momentum Dependent (TMD or k_t) Factorization
2. Introduction to Small-x Physics
   - BFKL evolution and Balitsky-Kovchegov evolution equations
   - McLerran-Venugopalan Model
3. Dihadron Correlations
   - Breaking down of the k_t factorization in di-jet production
   - Probing two fundamental gluon distributions
   - Gluon+Jet in pA

Deep inelastic scattering and Drell-Yan process

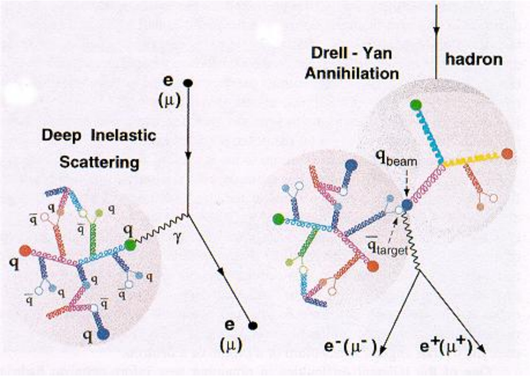

Light Cone coordinates and gauge

For a relativistic hadron moving in the $+z$ direction

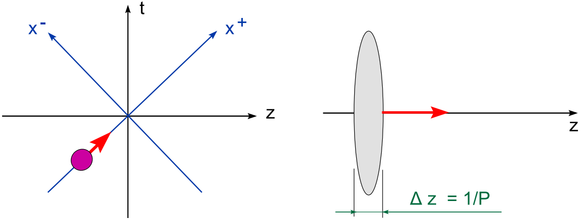

- In this frame, the momenta are defined

$$P^+ = \frac{1}{\sqrt{2}}(P^0 + P^3) \quad \text{and} \quad P^- = \frac{1}{\sqrt{2}}(P^0 - P^3) \to 0$$

- $P^2 = 2P^+P^- - P_\perp^2$
- Light cone gauge for a gluon with momentum $k^\mu = (k^+, k^-, k_\perp)$, the polarization vector reads

$$k^\mu \epsilon_\mu = 0 \Rightarrow \quad \epsilon = (\epsilon^+ = 0, \epsilon^- = \frac{\epsilon_\perp \cdot k_\perp}{k^+}, \epsilon_\perp^\pm) \quad \text{with} \quad \epsilon_\perp^\pm = \frac{1}{\sqrt{2}}(1, \pm i)$$

Deep inelastic scattering

Summary of DIS:

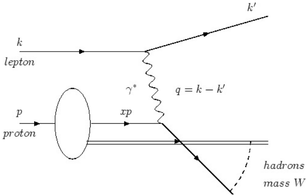

$$\frac{d\sigma}{dE' d\Omega} = \frac{\alpha_{\mathrm{em}^2}}{Q^4}\frac{E'}{E} L_{\mu\nu} W^{\mu\nu}$$

with $L_{\mu\nu}$ the leptonic tensor and $W^{\mu\nu}$ defined as

$$W^{\mu\nu} = \left(-g^{\mu\nu} + \frac{q_\mu q_\nu}{q^2}\right) W_1 + \frac{1}{m_p^2}\left(P^\mu - \frac{P\cdot q}{q^2} q^\mu\right)\left(P^\nu - \frac{P\cdot q}{q^2} q^\nu\right) W_2$$

Introduce the dimensionless structure function:

$$F_1 \equiv W_1 \quad \text{and} \quad F_2 \equiv \frac{Q^2}{2m_p x} W_2$$

$$\Rightarrow \frac{d\sigma}{dx dy} = \frac{\alpha_{\mathrm{em}}^2 4\pi s}{Q^4}\left[(1-y)F_2 + xy^2 F_1\right] \quad \text{with} \quad y = \frac{P\cdot q}{P\cdot k}.$$

Quark Parton Model: Callan-Gross relation

$$F_2(x) = 2xF_1(x) = \sum_q e_q^2 x\left[f_q(x) + f_{\bar{q}}(x)\right].$$

PENNSTATE 1855

Callan-Gross relation

Callan - Gross Relation

$$\left(\frac{d\sigma}{dq^2}\right)_{\text{Dirac}} = \frac{4\pi\alpha^2 z^2}{q^4}\left(\frac{E'}{E}\right)^2\left(\cos^2\frac{\theta}{2} + \frac{q^2}{2m^2}\sin^2\frac{\theta}{2}\right)$$

$$\left(\frac{d^2\sigma}{dq^2\,dx}\right)_{\text{inelastic}} = \frac{4\pi\alpha^2}{q^4}\frac{E'}{E}\left(F_2(x)\cos^2\frac{\theta}{2} + \frac{q^2}{2M^2x^2}2xF_1(x)\sin^2\frac{\theta}{2}\right)\frac{1}{x}$$

Electric Magnetic

$\frac{2xF_1(x)}{F_2(x)} = 1$ For spin $\frac{1}{2}$ partons

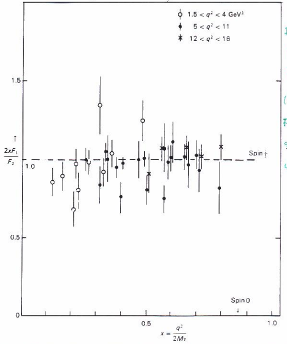

For spin 0 partons: $F_1 = 0$ (Remember: F_1 describes spin - spin interaction)

Figure 8.10 The ratio $2xF_1/F_2$ measured in SLAC electron-nucleon scattering experiments. For spin-$\frac{1}{2}$ partons, with $g = 2$, a ratio of unity is expected in the limit of large q^2—the Callan-Gross relation. (Data compiled from published SLAC data.)

=> quarks have spin $\frac{1}{2}$!

- The relation ($F_L = F_2 - 2xF_1$) follows from the fact that a spin-$\frac{1}{2}$ quark cannot absorb a longitudinally polarized vector boson.
- In contrast, spin-0 quark cannot absorb transverse bosons and so would give $F_1 = 0$.

Parton Density

The probabilistic interpretation of the parton density.

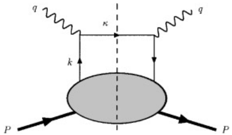

$$\Rightarrow \quad f_q(x) = \int \frac{\mathrm{d}\zeta^-}{4\pi} e^{ixP^+\zeta^-} \langle P \left| \bar{\psi}(0)\gamma^+\psi(0,\zeta^-) \right| P \rangle$$

Comments:

- Gauge link $\mathcal{L}$ is necessary to make the parton density gauge invariant.

$$\mathcal{L}(0,\zeta^-) = \mathcal{P}\exp\left(\int_0^{\zeta^-} \mathrm{d}s_\mu A^\mu\right)$$

- Choose light cone gauge $A^+ = 0$ and right path, one can eliminate the gauge link.
- Now we can interpret $f_q(x)$ as parton density in the light cone frame.
- Evolution of parton density: Change of resolution

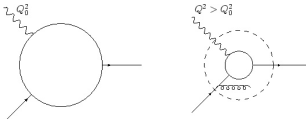

a) b)

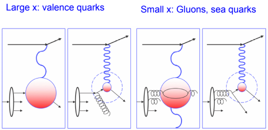

- At low-x, dominant channels are different.

Drell-Yan process

For lepton pair productions in hadron-hadron collisions:

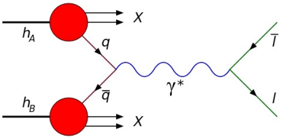

the cross section is

$$\frac{d\sigma}{dM^2 dY} = \sum_q x_1 f_q(x_1) x_2 f_{\bar{q}}(x_2) \frac{1}{3} e_q^2 \frac{4\pi\alpha^2}{3M^4} \quad \text{with} \quad Y = \frac{1}{2} \ln \frac{x_1}{x_2}.$$

- Collinear factorization proof shows that $f_q(x)$ involved in DIS and Drell-Yan process are the same.
- At low-x and high energy, the dominant channel is $qg \to q\gamma^*(l^+ l^-)$.

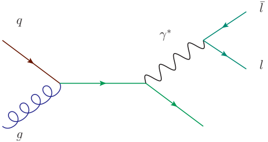

PENNSTATE 1855

Splitting function

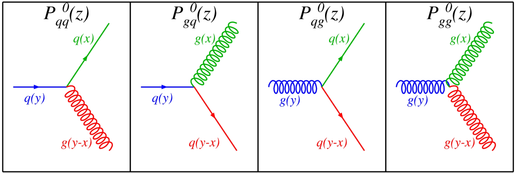

$$\mathcal{P}^0_{qq}(\xi) = \frac{1+\xi^2}{(1-\xi)_+} + \frac{3}{2}\delta(1-\xi),$$

$$\mathcal{P}^0_{gq}(\xi) = \frac{1}{\xi}\left[1+(1-\xi)^2\right],$$

$$\mathcal{P}^0_{qg}(\xi) = \left[(1-\xi)^2+\xi^2\right],$$

$$\mathcal{P}^0_{gg}(\xi) = 2\left[\frac{\xi}{(1-\xi)_+} + \frac{1-\xi}{\xi} + \xi(1-\xi)\right] + \left(\frac{11}{6} - \frac{2N_f T_R}{3N_c}\right)\delta(1-\xi).$$

- $\xi = z = \frac{x}{y}$.
- $\int_0^1 \frac{\mathrm{d}\xi f(\xi)}{(1-\xi)_+} = \int_0^1 \frac{\mathrm{d}\xi[f(\xi)-f(1)]}{1-\xi} \Rightarrow \int_0^1 \frac{\mathrm{d}\xi}{(1-\xi)_+} = 0$

Derivation of $\mathcal{P}^0_{qq}(\xi)$

The real contribution:

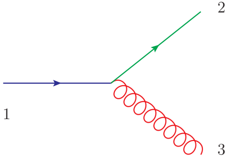

$$k_1 = (P^+, 0, 0_\perp) \quad ; \quad k_2 = (\xi P^+, \frac{k_\perp^2}{\xi P^+}, k_\perp)$$

$$k_3 = ((1-\xi)P^+, \frac{k_\perp^2}{(1-\xi)P^+}, -k_\perp) \quad \epsilon_3 = (0, -\frac{2k_\perp \cdot \epsilon_\perp^{(3)}}{(1-\xi)P^+}, \epsilon_\perp^{(3)})$$

$$|V_{q\to qg}|^2 = \frac{1}{2}\mathrm{Tr}\,(\not{k}_2\gamma_\mu\not{k}_1\gamma_\nu)\sum \epsilon_3^{*\mu}\epsilon_3^\nu = \frac{2k_\perp^2}{\xi(1-\xi)}\,\frac{1+\xi^2}{1-\xi}$$

$$\Rightarrow \qquad \mathcal{P}_{qq}(\xi) = \frac{1+\xi^2}{1-\xi} \quad (\xi < 1)$$

- Including the virtual graph 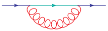 , use $\int_a^1 \frac{d\xi g(\xi)}{(1-\xi)_+} = \int_a^1 \frac{d\xi g(\xi)}{1-\xi} - g(1)\int_0^1 \frac{d\xi}{1-\xi}$

$$\frac{\alpha_s C_F}{2\pi}\left[\int_x^1 \frac{d\xi}{\xi} q(x/\xi)\frac{1+\xi^2}{1-\xi} - q(x)\int_0^1 d\xi \frac{1+\xi^2}{1-\xi}\right]$$

$$= \quad \frac{\alpha_s C_F}{2\pi}\left[\int_x^1 \frac{d\xi}{\xi} q(x/\xi)\frac{1+\xi^2}{(1-\xi)_+} - q(x)\underbrace{\int_0^1 d\xi \frac{1+\xi^2}{(1-\xi)_+}}_{=-\frac{3}{2}}\right].$$

Derivation of $\mathcal{P}^0_{qq}(\xi)$

The real contribution:

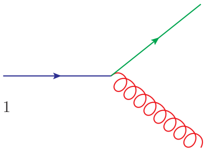

$$k_1 = (P^+, 0, 0_\perp) \quad ; \quad k_2 = (\xi P^+, \frac{k_\perp^2}{\xi P^+}, k_\perp)$$

$$k_3 = ((1-\xi)P^+, \frac{k_\perp^2}{(1-\xi)P^+}, -k_\perp) \quad \epsilon_3 = (0, -\frac{2k_\perp \cdot \epsilon_\perp^{(3)}}{(1-\xi)P^+}, \epsilon_\perp^{(3)})$$

$$|V_{q\to qg}|^2 = \frac{1}{2}\mathrm{Tr}\,(\not{k}_2\gamma_\mu \not{k}_1 \gamma_\nu) \sum \epsilon_3^{*\mu}\epsilon_3^\nu = \frac{2k_\perp^2}{\xi(1-\xi)} \frac{1+\xi^2}{1-\xi}$$

$$\Rightarrow \qquad \mathcal{P}_{qq}(\xi) = \frac{1+\xi^2}{1-\xi} \quad (\xi < 1)$$

- Regularize $\frac{1}{1-\xi}$ to $\frac{1}{(1-\xi)_+}$ by including the divergence from the virtual graph.
- Probability conservation:

$$P_{qq} + \mathrm{d}P_{qq} = \delta(1-\xi) + \frac{\alpha_s C_F}{2\pi}\mathcal{P}^0_{qq}(\xi)dt \quad \text{and} \quad \int_0^1 \mathrm{d}\xi \mathcal{P}_{qq}(\xi) = 0,$$

$$\Rightarrow \mathcal{P}_{qq}(\xi) = \frac{1+\xi^2}{(1-\xi)_+} + \frac{3}{2}\delta(1-\xi) = \left(\frac{1+\xi^2}{1-\xi}\right)_+ .$$

PENNSTATE 1855

Derivation of $\mathcal{P}^0_{gg}(\xi)$

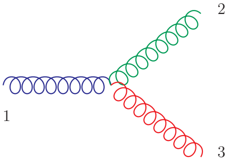

$$k_1 = (P^+, 0, 0_\perp) \quad \epsilon_1 = (0, 0, \epsilon_\perp^{(1)}) \quad \text{with} \quad \epsilon_\perp^\pm = \frac{1}{\sqrt{2}}(1, \pm i)$$

$$k_2 = (\xi P^+, \frac{k_\perp^2}{\xi P^+}, k_\perp) \quad \epsilon_2 = (0, \frac{2k_\perp \cdot \epsilon_\perp^{(2)}}{\xi P^+}, \epsilon_\perp^{(2)})$$

$$k_3 = ((1-\xi)P^+, \frac{k_\perp^2}{(1-\xi)P^+}, -k_\perp) \quad \epsilon_3 = (0, -\frac{2k_\perp \cdot \epsilon_\perp^{(3)}}{(1-\xi)P^+}, \epsilon_\perp^{(3)})$$

$$V_{g\to gg} = (k_1 + k_3)\cdot \epsilon_2 \epsilon_1 \cdot \epsilon_3 + (k_2 - k_3)\cdot \epsilon_1 \epsilon_2 \cdot \epsilon_3 - (k_1 + k_2)\cdot \epsilon_3 \epsilon_1 \cdot \epsilon_2$$

$$\Rightarrow \qquad |V_{g\to gg}|^2 = |V_{+++}|^2 + |V_{+-+}|^2 + |V_{++-}|^2 = 4k_\perp^2 \frac{[1-\xi(1-\xi)]^2}{\xi^2(1-\xi)^2}$$

$$\Rightarrow \qquad \mathcal{P}_{gg}(\xi) = 2\left[\frac{1-\xi}{\xi} + \frac{\xi}{1-\xi} + \xi(1-\xi)\right] \quad (\xi < 1)$$

- Regularize $\frac{1}{1-\xi}$ to $\frac{1}{(1-\xi)_+}$
- Momentum conservation:

$$\int_0^1 d\xi\, \xi\, [\mathcal{P}_{qq}(\xi) + \mathcal{P}_{gq}(\xi)] = 0 \qquad \int_0^1 d\xi\, \xi\, [2\mathcal{P}_{qg}(\xi) + \mathcal{P}_{gg}(\xi)] = 0,$$

$\Rightarrow$ the terms which is proportional to $\delta(1-\xi)$.

- HW: derive other splitting functions.

DGLAP equation

In the leading logarithmic approximation with $t = \ln \mu^2$, the parton distribution and fragmentation functions follow the DGLAP[Dokshitzer, Gribov, Lipatov, Altarelli, Parisi, 1972-1977] evolution equation as follows:

$$\frac{\mathrm{d}}{\mathrm{d}t}\left[\begin{array}{c} q(x,\mu) \\ g(x,\mu) \end{array}\right] = \frac{\alpha(\mu)}{2\pi}\int_x^1 \frac{d\xi}{\xi}\left[\begin{array}{cc} C_F P_{qq}(\xi) & T_R P_{qg}(\xi) \\ C_F P_{gq}(\xi) & N_c P_{gg}(\xi) \end{array}\right]\left[\begin{array}{c} q(x/\xi,\mu) \\ g(x/\xi,\mu) \end{array}\right],$$

and

$$\frac{\mathrm{d}}{\mathrm{d}t}\left[\begin{array}{c} D_{h/q}(z,\mu) \\ D_{h/g}(z,\mu) \end{array}\right] = \frac{\alpha(\mu)}{2\pi}\int_z^1 \frac{d\xi}{\xi}\left[\begin{array}{cc} C_F P_{qq}(\xi) & C_F P_{gq}(\xi) \\ T_R P_{qg}(\xi) & N_c P_{gg}(\xi) \end{array}\right]\left[\begin{array}{c} D_{h/q}(z/\xi,\mu) \\ D_{h/g}(z/\xi,\mu) \end{array}\right],$$

Comments:

- In the double asymptotic limit, $Q^2 \to \infty$ and $x \to 0$, the gluon distribution can be solved analytically and cast into

$$xg(x,\mu^2) \simeq exp\left(2\sqrt{\frac{\alpha_s N_c}{\pi}\ln\frac{1}{x}\ln\frac{\mu^2}{\mu_0^2}}\right) \quad \text{Fixed coupling}$$

$$xg(x,\mu^2) \simeq exp\left(2\sqrt{\frac{N_c}{\pi b}\ln\frac{1}{x}\ln\frac{\ln\mu^2/\Lambda^2}{\ln\mu_0^2/\Lambda^2}}\right) \quad \text{Running coupling}$$

- The full DGLAP equation can be solved numerically.

Collinear Factorization at NLO

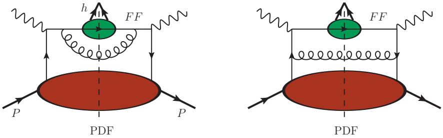

Use $\overline{\text{MS}}$ scheme ($\frac{1}{\hat{\epsilon}} = \frac{1}{\epsilon} + \ln 4\pi - \gamma_E$) and dimensional regularization, DGLAP equation reads

$$\begin{bmatrix} q(x,\mu) \\ g(x,\mu) \end{bmatrix} = \begin{bmatrix} q^{(0)}(x) \\ g^{(0)}(x) \end{bmatrix} - \frac{1}{\hat{\epsilon}} \frac{\alpha(\mu)}{2\pi} \int_x^1 \frac{d\xi}{\xi} \begin{bmatrix} C_F P_{qq}(\xi) & T_R P_{qg}(\xi) \\ C_F P_{gq}(\xi) & N_c P_{gg}(\xi) \end{bmatrix} \begin{bmatrix} q(x/\xi) \\ g(x/\xi) \end{bmatrix},$$

and

$$\begin{bmatrix} D_{h/q}(z,\mu) \\ D_{h/g}(z,\mu) \end{bmatrix} = \begin{bmatrix} D_{h/q}^{(0)}(z) \\ D_{h/g}^{(0)}(z) \end{bmatrix} - \frac{1}{\hat{\epsilon}} \frac{\alpha(\mu)}{2\pi} \int_z^1 \frac{d\xi}{\xi} \begin{bmatrix} C_F P_{qq}(\xi) & C_F P_{gq}(\xi) \\ T_R P_{qg}(\xi) & N_c P_{gg}(\xi) \end{bmatrix} \begin{bmatrix} D_{h/q}(z/\xi) \\ D_{h/g}(z/\xi) \end{bmatrix}.$$

- Soft divergence cancels between real and virtual diagrams;
- Gluon collinear to the initial state quark ⇒ parton distribution function; Gluon collinear to the final state quark ⇒ fragmentation function. KLN theorem does not apply.
- Other kinematical region of the radiated gluon contributes to the NLO ($\mathcal{O}(\alpha_s)$ correction) hard factor.

DGLAP evolution

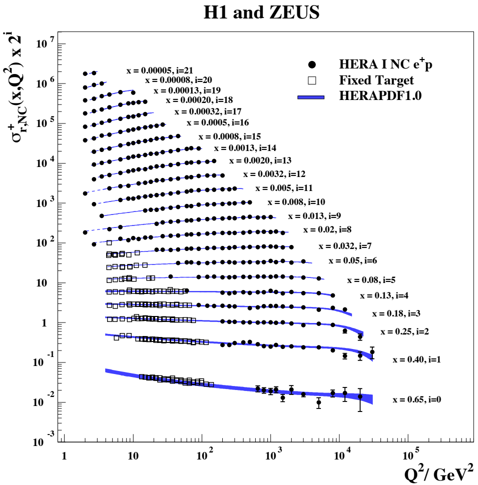

DGLAP evolution

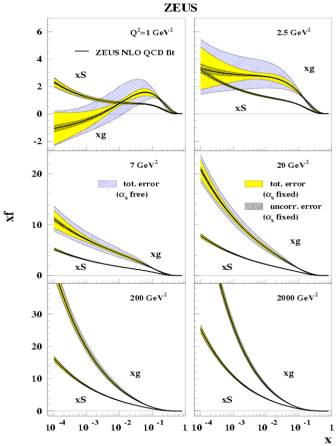

- NLO DGLAP fit yields negative gluon distribution at low Q^2 and low x.
- Does this mean there is no gluons in that region? No

Phase diagram in QCD

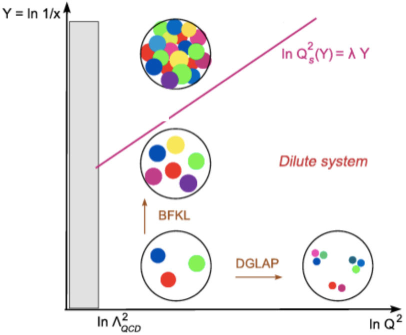

- Low Q^2 and low x region $\Rightarrow$ saturation region.
- Use BFKL equation and BK equation instead of DGLAP equation.
- BK equation is the non-linear small-x evolution equation which describes the saturation physics.

Collinear Factorization vs $k_\perp$ Factorization

Collinear Factorization

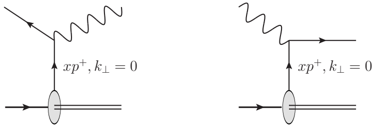

$k_\perp$ Factorization(Spin physics and saturation physics)

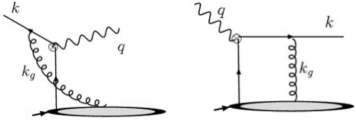

- The incoming partons carry no $k_\perp$ in the Collinear Factorization.
- In general, there is intrinsic $k_\perp$. It can be negligible for partons in protons, but should be taken into account for the case of nucleus target with large number of nucleons ($A \to \infty$).
- $k_\perp$ Factorization: High energy evolution with $k_\perp$ fixed.
- Initial and final state interactions yield different gauge links. (Process dependent)
- In collinear factorization, gauge links all disappear in the light cone gauge, and PDFs are universal.
- Other approaches, such as nuclear modification and higher twist approach. (See last year's lecture.)

k_t dependent parton distributions

The unintegrated quark distribution

$$f_q(x,k_\perp) = \int \frac{d\xi^- d^2\xi_\perp}{4\pi(2\pi)^2} e^{ixP^+\xi^- + i\xi_\perp\cdot k_\perp} \langle P \left| \bar{\psi}(0)\mathcal{L}^\dagger(0)\gamma^+\mathcal{L}(\xi^-,\xi_\perp)\psi(\xi_\perp,\xi^-) \right| P\rangle$$

as compared to the integrated quark distribution

$$f_q(x) = \int \frac{d\xi^-}{4\pi} e^{ixP^+\xi^-} \langle P \left| \bar{\psi}(0)\gamma^+\mathcal{L}(\xi^-)\psi(0,\xi^-) \right| P\rangle$$

- The dependence of $\xi_\perp$ in the definition.
- Gauge invariant definition.
- Light-cone gauge together with proper boundary condition $\Rightarrow$ parton density interpretation.
- The gauge links come from the resummation of multiple gluon interactions.
- Gauge links may vary among different processes.

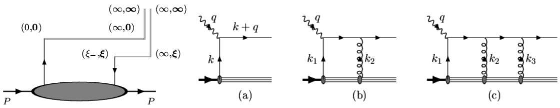

PENNSTATE 1855

TMD factorization

One-loop factorization:

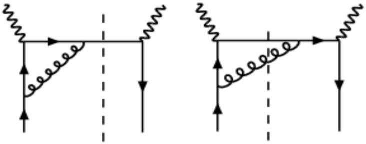

For gluon with momentum k

- k is collinear to initial quark $\Rightarrow$ parton distribution function;
- k is collinear to the final state quark $\Rightarrow$ fragmentation function.
- k is soft divergence (sometimes called rapidity divergence) $\Rightarrow$ Wilson lines (Soft factor) or small-x evolution for gluon distribution.
- Other kinematical region of the radiated gluon contributes to the NLO ($\mathcal{O}(\alpha_s)$ correction) hard factor.
- See new development in Collins' book.

PENNSTATE

Deep into low-x region of Protons

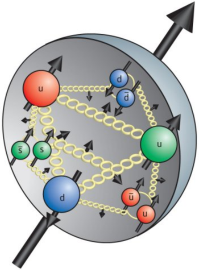

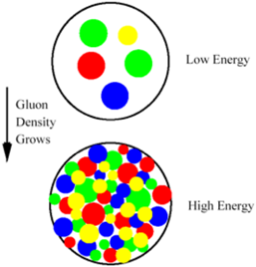

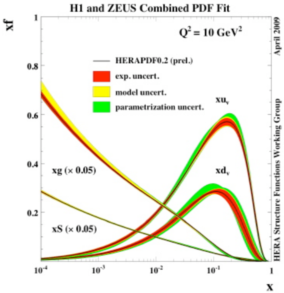

- Gluon splitting functions ($\mathcal{P}^0_{qq}(\xi)$ and $\mathcal{P}^0_{gg}(\xi)$) have $1/(1-\xi)$ singularities.
- Partons in the low-x region is dominated by gluons.
- Resummation of the $\alpha_s \ln \frac{1}{x}$.

PENNSTATE
1855

Dual Descriptions of Deep Inelastic Scattering

[A. Mueller, 01; Parton Saturation-An Overview]

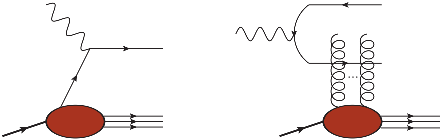

Bjorken frame   Dipole frame

Bjorken frame

$$F_2(x,Q^2) = \sum_q e_q^2 x \left[f_q(x,Q^2) + f_{\bar{q}}(x,Q^2) \right].$$

Dipole frame

$$F_2(x,Q^2) = \sum_f e_f^2 \frac{Q^2}{4\pi^2\alpha_{\rm em}} \int_0^1 {\rm d}z \int {\rm d}^2x_\perp {\rm d}^2y_\perp \left[|\psi_T(z,r_\perp,Q)|^2 + |\psi_L(z,r_\perp,Q)|^2 \right] \times [1 - S(r_\perp)], \quad \text{with} \quad r_\perp = x_\perp - y_\perp.$$

- Bjorken: the partonic picture of a hadron is manifest. Saturation shows up as a limit on the occupation number of quarks and gluons.
- Dipole: the partonic picture is no longer manifest. Saturation appears as the unitarity limit for scattering. Convenient to resum the multiple gluon interactions.

BFKL evolution

[Balitsky, Fadin, Kuraev, Lipatov;74] The infrared sensitivity of Bremsstrahlung favors the emission of small-x gluons:

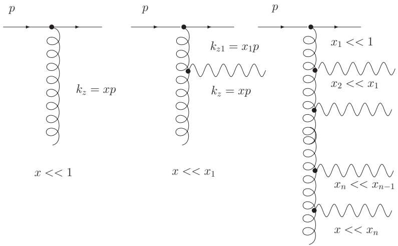

Probability of emission:

$$dp \sim \alpha_s N_c \frac{dk_z}{k_z} = \alpha_s N_c \frac{dx}{x}$$

In small-x limit and Leading log approximation:

$$p \sim \sum_{n=0}^{\infty} \alpha_s^n N_c^n \int_x^1 \frac{dx_n}{x_n} \cdots \int_{x_2}^1 \frac{dx_1}{x_1} \sim \exp\left(\alpha_s N_c \ln \frac{1}{x}\right)$$

- Exponential growth of the amplitude as function of rapidity;
- As compared to DGLAP which resums $\alpha_s N_c \ln \frac{1}{x} \ln \frac{\mu^2}{\mu_0^2}$.

Derivation of BFKL evolution

Dipole model. [Mueller, 94]
Consider a Bremsstrahlung emission of soft gluon $z_g \ll 1$,

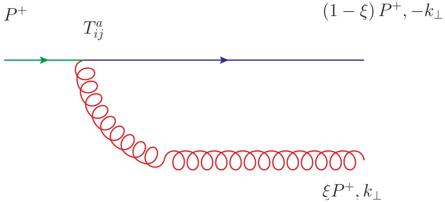

and use LC gauge $\epsilon = (\epsilon^+ = 0, \epsilon^- = \frac{\epsilon_\perp \cdot k_\perp}{k^+}, \epsilon_\perp^\pm)$

$$\mathcal{M}(k_\perp) = -2igT^a \frac{\epsilon_\perp \cdot k_\perp}{k_\perp^2}$$

- $q \to qg$ vertex and Energy denominator.
- Take the limit $k_g^+ \to 0$.
- Similar to the derivation of $\mathcal{P}_{qq}(\xi)$.

The dipole splitting kernal

The Bremsstrahlung amplitude in the coordinate space

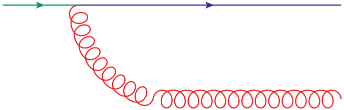

$$\mathcal{M}(x_\perp - z_\perp) = \int \mathrm{d}^2 k_\perp e^{ik_\perp \cdot (x_\perp - z_\perp)} \mathcal{M}(k_\perp)$$

$$\text{Use} \quad \int \mathrm{d}^2 k_\perp \frac{\epsilon_\perp \cdot k_\perp}{k_\perp^2} e^{ik_\perp \cdot b_\perp} = 2\pi i \frac{\epsilon_\perp \cdot b_\perp}{b_\perp^2},$$

$$\Rightarrow \qquad \mathcal{M}(x_\perp - z_\perp) = 4\pi g T^a \frac{\epsilon_\perp \cdot (x_\perp - z_\perp)}{(x_\perp - z_\perp)^2}$$

The dipole splitting kernal

Consider soft gluon emission from a color dipole in the coordinate space $(x_\perp, y_\perp)$

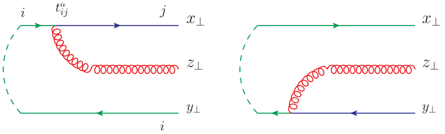

$$\mathcal{M}(x_\perp, z_\perp, y_\perp) = 4\pi g T^a \left[\frac{\epsilon_\perp \cdot (x_\perp - z_\perp)}{(x_\perp - z_\perp)^2} - \frac{\epsilon_\perp \cdot (y_\perp - z_\perp)}{(y_\perp - z_\perp)^2} \right] \Rightarrow$$

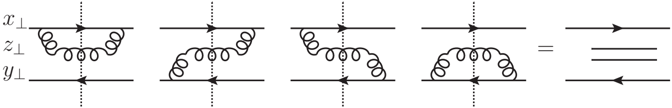

$$= \frac{\alpha_s N_c}{2\pi^2} \frac{(x_\perp - y_\perp)^2}{(x_\perp - z_\perp)^2 (y_\perp - z_\perp)^2}$$

- The probability of dipole splitting at large N_c limit

$$dP_{\text{splitting}} = \frac{\alpha_s N_c}{2\pi^2} \frac{(x_\perp - y_\perp)^2}{(x_\perp - z_\perp)^2 (x_\perp - z_\perp)^2} \mathrm{d}^2 z_\perp \mathrm{d}Y \quad \text{with} \quad \mathrm{d}Y = \frac{\mathrm{d}k_g^+}{k_g^+}$$

- Gluon splitting $\Leftrightarrow$ Dipole splitting.

BFKL evolution in Mueller's dipole model

[Mueller; 94] In large N_c limit, BFKL evolution can be viewed as dipole branching in a fast moving $q\bar{q}$ dipole in coordinate space:

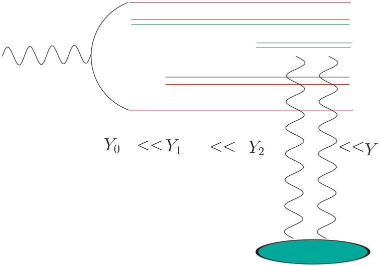

$n(r, Y)$ dipoles of size r.

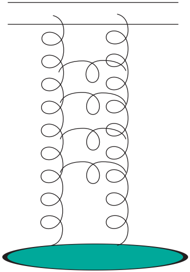

BFKL Pomeron

The T matrix ($T \equiv 1 - S$ with S being the scattering matrix) basically just counts the number of dipoles of a given size,

$$T(r, Y) \sim \alpha_s^2 n(r, Y)$$

- The probability of emission is $\bar{\alpha}_s \frac{(x-y)^2}{(x-z)^2(z-y)^2}$;
- Assume independent emissions with large separation in rapidity.

BFKL equation

Consider a slight change in rapidity and the Bremsstrahlung emission of soft gluon (dipole splitting)

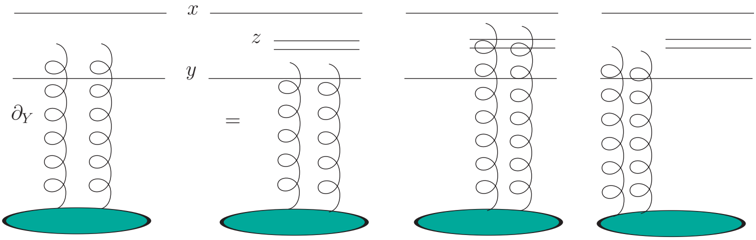

$$\partial_Y T(x, y; Y) = \frac{\bar{\alpha}_s}{2\pi} \int d^2z \frac{(x-y)^2}{(x-z)^2(z-y)^2} \left[T(x, z; Y) + T(z, y; Y) - T(x, y; Y)\right]$$

Kovchegov equation

[Kovchegov; 99] [Mueller; 01] Including non-linear effects: ($T \equiv 1 - S$)

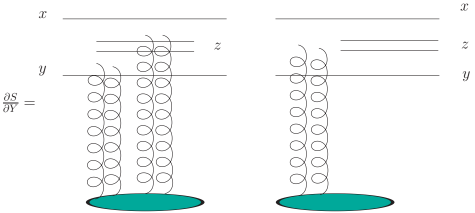

$$\partial_Y S(x-y;Y) = \frac{\alpha N_c}{2\pi^2}\int d^2z \frac{(x-y)^2}{(x-z)^2(z-y)^2}\left[S(x-z;Y)S(z-y;Y) - S(x-y;Y)\right]$$

$$\partial_Y T(x-y;Y) = \frac{\alpha N_c}{2\pi^2}\int d^2z \frac{(x-y)^2}{(x-z)^2(z-y)^2} \times \left[T(x-z;Y) + T(z-y;Y) - T(x-y;Y) - \underbrace{T(x-z;Y)T(z-y;Y)}_{\text{saturation}}\right]$$

- Linear BFKL evolution results in fast energy evolution.
- Non-linear term $\Rightarrow$ fixed point ($T = 1$) and unitarization, and thus saturation.

Phase diagram in QCD

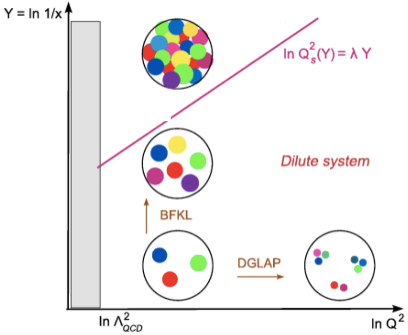

- Low Q^2 and low x region $\Rightarrow$ saturation region.
- Balitsky-Kovchegov equation is the non-linear small-x evolution equation which describes the saturation physics.

PENNSTATE

Balitsky-Kovchegov equation vs F-KPP equation

[Munier, Peschanski, 03] Consider the case with fixed impact parameter, namely, T_{xy} is only function of $r = x - y$. Then, transforming the B-K equation into momentum space:

BK equation: $\boxed{\partial_Y T = \bar{\alpha}\chi_{\mathrm{BFKL}}(-\partial_\rho)T - \bar{\alpha}T^2}$ with $\boxed{\bar{\alpha} = \frac{\alpha N_c}{\pi}}$

Diffusion approximation $\Rightarrow$

F-KPP equation: $\boxed{\partial_t u(x,t) = \partial_x^2 u(x,t) + u(x,t) - u^2(x,t)}$

- $u \Rightarrow T$, $\bar{\alpha}Y \Rightarrow t$, $\varrho = \log(k^2/k_0^2) \Rightarrow x$, with k_0 being the reference scale;
- B-K equation lies in the same universality class as the F-KPP [Fisher-Kolmogrov-Petrovsky-Piscounov; 1937] equation.
- F-KPP equation admits traveling wave solution $u = u\,(x - vt)$ with minimum velocity;
- the non-linear term saturates the solution in the infrared.

Balitsky-Kovchegov equation vs F-KPP equation

BK equation: $\boxed{\partial_Y T = \bar{\alpha}\chi_{\mathrm{BFKL}}(-\partial_\varrho)T - \bar{\alpha}T^2}$

The linear part of its solution $T_{\mathrm{lin}}(k, Y)$ is a superposition of waves:

$$T_{\mathrm{lin}}(k, Y) = \int_{c-i\infty}^{c+i\infty} \frac{d\gamma}{2i\pi} \exp\left[-\gamma\left(\varrho - \bar{\alpha}v(\gamma)Y\right)\right] T_0(\gamma)$$

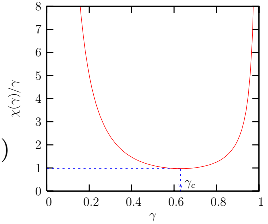

- $T_0(\gamma)$: the initial condition,
- Each wave has a different speed $v(\gamma)$ given by $v(\gamma) = \frac{\chi(\gamma)}{\gamma}$ with $\chi(\gamma) = \psi(1) - \frac{1}{2}\psi(\gamma) - \frac{1}{2}\psi(1-\gamma)$ and $\psi(\gamma) = \frac{d}{d\gamma}\log[\Gamma(\gamma)]$ being the digamma function.
- [Mueller, Triantafyllopoulos; 02]Using saddle point approximation, and requiring exponent vanishes at the saddle point. one gets $\gamma_c = 0.63$. This corresponds to an anomalous dimension 0.37.
- The wave speed $v(\gamma)$ is minimized at $\gamma_c = 0.63$. γ_c is selected by exponential growth and saturation.

Geometrical scaling

Geometrical scaling in DIS:

$$\begin{aligned} T(r,Y) &= T\left[r^2 Q_s^2(Y)\right] \\ &= \left[r^2 Q_s^2(Y)\right]^{\gamma_c} \underbrace{\exp\left[-\frac{\log^2\left(r^2 Q_s^2(Y)\right)}{2\chi''(\gamma_c)\,\bar{\alpha}Y}\right]}_{\text{Scaling window}} \end{aligned}$$

- All data of $\sigma_{tot}^{\gamma^* p}$ when $x \leq 0.01$ and $\frac{1}{r^2} = Q^2 \leq 450GeV^2$ plotting as function of $\tau = Q^2/Q_s^2$ falls on a curve, where $Q_s^2 = \left(\frac{x_0}{x}\right)^{0.29} GeV^2$ with $x_0 = 3 \times 10^{-4}$;
- scaling window: $|\log\left(r^2 Q_s^2(Y)\right)| \ll \sqrt{2\chi''(\gamma_c)\,\bar{\alpha}Y}$.

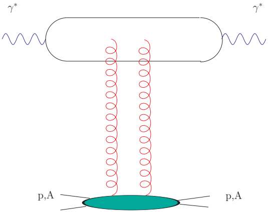

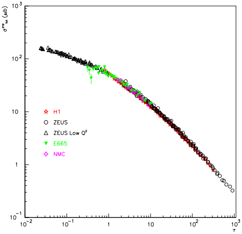

[Golec-Biernat, Stasto, Kwiecinski; 01]

McLerran-Venugopalan Model

In QCD, the McLerran-Venugopalan Model describes high density gluon distribution in a relativistic large nucleus ($A \gg 1$) by solving the classical Yang-Mills equation:

$$[D_\mu, F^{\mu\nu}] = gJ^\nu \quad \text{with} \quad J^\nu = \delta^{\nu+}\rho_a(x^-, x_\perp)T^a, \quad \text{COV gauge} \Rightarrow -\nabla_\perp^2 A^+ = g\rho.$$

To solve the above equation, we define the Green's function

$$\nabla_{z_\perp}^2 G(x_\perp - z_\perp) = \delta^{(2)}(x_\perp - z_\perp) \quad \Rightarrow \quad G(x_\perp - z_\perp) = -\int \frac{\mathrm{d}^2 k_\perp}{(2\pi)^2} \frac{e^{ik_\perp\cdot(x_\perp - z_\perp)}}{k_\perp^2}$$

MV model assumes that the density of color charges follows a Gaussian distribution

$$W[\rho] = \exp\left[-\int \mathrm{d}z^- \mathrm{d}^2 z_\perp \frac{\rho_a(z^-, z_\perp)\rho_a(z^-, z_\perp)}{2\mu^2(z^-)}\right].$$

With such a weight, average of two color sources is

$$\langle \rho_a \rho_b \rangle = \int \mathcal{D}[\rho] W[\rho] \rho_a(x^-, x_\perp)\rho_b(y^-, y_\perp) = \mu^2(x^-)\delta_{ab}\delta(x^- - y^-)\delta(x_\perp - y_\perp).$$

PENNSTATE

Dipole amplitude in MV model

The Wilson line [F. Gelis, A. Peshier, 01]

$$U(x_\perp) = \mathcal{P}\exp\left[-ig^2\int \mathrm{d}z^- \mathrm{d}^2 z_\perp G\left(x_\perp - z_\perp\right)\rho\left(z^-, z_\perp\right)\right]$$

$U(x_\perp) \equiv$ 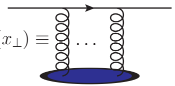

$S(x_\perp, y_\perp) \equiv \frac{1}{N_c}\mathrm{Tr}U(x_\perp)U^\dagger(y_\perp)$ 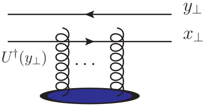

Use gaussian approximation to pair color charges:

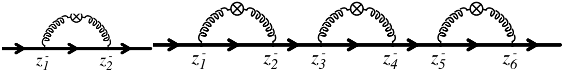

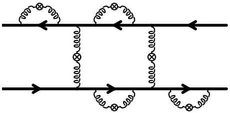

$$\Rightarrow S(x_\perp, y_\perp) \simeq \exp\left\{-\frac{\mu_s^2}{4}\int \mathrm{d}^2 z_\perp \left[G\left(x_\perp - z_\perp\right) - G\left(y_\perp - z_\perp\right)\right]^2\right\}$$

$$\simeq \exp\left[-\frac{1}{4}Q_s^2\left(x_\perp - y_\perp\right)^2\right] \Leftarrow \text{GBW model}$$

PENNSTATE

- Quadrupoles $\frac{1}{N_c}\mathrm{Tr}U_1U_2^\dagger U_3U_4^\dagger$ and Sextupoles $\frac{1}{N_c}\mathrm{Tr}U_1U_2^\dagger U_3U_4^\dagger U_5U_6^\dagger\dots$

Golec-Biernat Wusthoff model and Geometrical Scaling

[Golec-Biernat, Wusthoff,; 98], [Golec-Biernat, Stasto, Kwiecinski; 01]

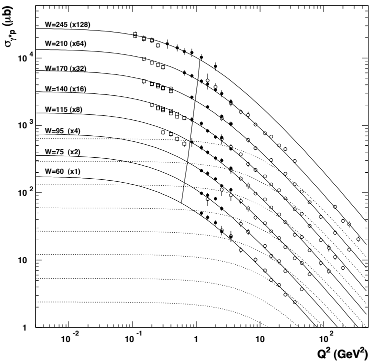

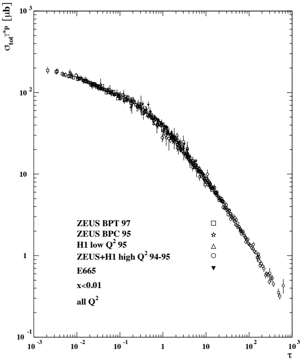

- The dipole amplitude in the GBW model

$$S_{q\bar{q}}(r_\perp) = \exp[-\frac{Q_s^2 r_\perp^2}{4}]$$

with $Q_s^2(x) = Q_{s0}^2(x_0/x)^\lambda$ where $Q_{s0} = 1\text{GeV}$, $x = 3.04 \times 10^{-3}$ and $\lambda = 0.288$.

K_t Factorization "expectation"

Consider the inclusive production of two high-transverse-momentum back-to-back particles in hadron-hadron collisions, i.e., in the process:

$$H_1 + H_2 \to H_3 + H_4 + X.$$

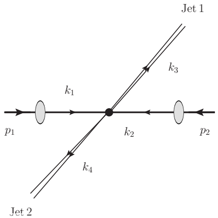

The standard k_t factorization "expectation" is:

$$\boxed{E_3 E_4 \frac{\mathrm{d}\sigma}{\mathrm{d}^3 p_3 \mathrm{d}^3 p_4} = \sum \int \mathrm{d}\hat{\sigma}_{i+j\to k+l+X} f_{i/1} f_{j/2} d_{3/k} d_{4/l} + \cdots}$$

- Convolution of $\mathrm{d}\hat{\sigma}$ with $f\,(x, k_\perp)$ and $d(z)$.
- Factorization $\Leftrightarrow$ Factorization formula + Universality
- Only Drell-Yan process is proved for factorization in hadron-hadron collisions. [Bodwin; 85, 86], [Collins, Soper, Sterman; 85, 88].

PENNSTATE

Breaking down of the k_t factorization in di-hadron production

- [Bacchetta, Bomhof, Mulders and Pijlman; 04-06] Wilson lines approach
  Studies of Wilson-line operators show that the TMD parton distributions are not generally process-independent due to the complicated combinantion of initial and final state interactions. TMD PDFs admit process dependent Wilson lines.
- [Collins, Qiu; 07], [Collins; 07], [Vogelsang, Yuan; 07] and [Rogers, Mulders; 10]
  Scalar QED models and its generalization to QCD (Counterexample to Factorization)

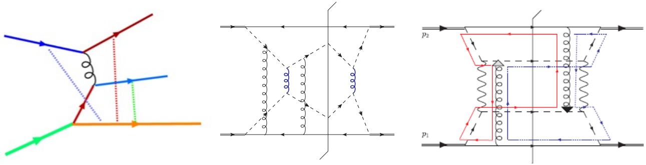

- $\mathcal{O}(g^2)$ calculation shows non-vanishing anomalous terms with respect to standard factorization.
- Remarks: k_t factorization is violated in di-jet production; TMD parton distributions are non-universal.
- Things get worse: For *pp* and *AA* collisions, no factorization formula at all for dijet production.

Why is the di-jet production process special?

Initial state interactions and/or final state interactions

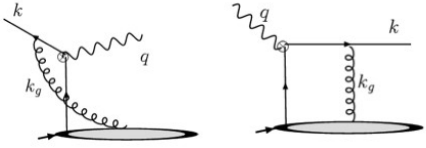

- In Drell-Yan process, there are only initial state interactions.

$$\int_{-\infty}^{+\infty} \mathrm{d}k_g^+ \frac{i}{-k_g^+ - i\epsilon} A^+(k_g) = \int_0^{-\infty} \mathrm{d}\zeta^- A^+(\zeta^-)$$

Eikonal approximation $\Longrightarrow$ gauge links.

- In DIS, there are only final state interactions.

$$\int_{-\infty}^{+\infty} \mathrm{d}k_g^+ \frac{i}{-k_g^+ + i\epsilon} A^+(k_g) = \int_0^{+\infty} \mathrm{d}\zeta^- A^+(\zeta^-)$$

Eikonal approximation $\Longrightarrow$ gauge links.

- However, there are both initial state interactions and final state interactions in the di-jet process.

Forward observables at pA collisions

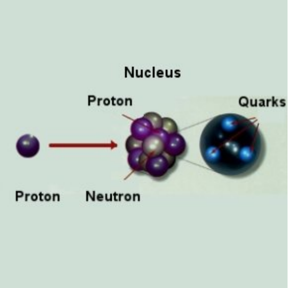

Why pA collisions?

- For pA (dilute-dense system) collisions, there is an effective k_t factorization.

$$\frac{d\sigma^{pA\to qfX}}{d^2P_\perp d^2q_\perp dy_1 dy_2} = x_p q(x_p,\mu^2) x_A f(x_A, q_\perp^2) \frac{1}{\pi}\frac{d\hat{\sigma}}{d\hat{t}}.$$

- For dijet processes in pp, AA collisions, there is no k_t factorization[Collins, Qiu, 08],[Rogers, Mulders; 10].

Why forward?

- At forward rapidity y, $x_p \propto e^y$ is large, while $x_A \propto e^{-y}$ is small.
- Ideal place to find gluon saturation in the target nucleus.

A Tale of Two Gluon Distributions

In small-x physics, two gluon distributions are widely used:[Kharzeev, Kovchegov, Tuchin; 03]
I. Weizsäcker Williams gluon distribution ([KM, 98'] and MV model):

$$xG^{(1)} = \frac{S_\perp}{\pi^2\alpha_s}\frac{N_c^2-1}{N_c} \Leftarrow$$
$$\times \int \frac{d^2r_\perp}{(2\pi)^2}\frac{e^{-ik_\perp\cdot r_\perp}}{r_\perp^2}\left(1-e^{-\frac{r_\perp^2 Q_{sg}^2}{2}}\right)$$

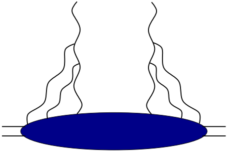

II. Color Dipole gluon distributions:

$$xG^{(2)} = \frac{S_\perp N_c}{2\pi^2\alpha_s}k_\perp^2 \Leftarrow$$
$$\times \int \frac{d^2r_\perp}{(2\pi)^2}e^{-ik_\perp\cdot r_\perp}e^{-\frac{r_\perp^2 Q_{sq}^2}{4}}$$

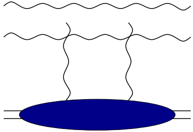

Remarks:

- The WW gluon distribution simply counts the number of gluons.
- The Color Dipole gluon distribution often appears in calculations.
- Does this mean that gluon distributions are non-universal? Answer: Yes and No!

PENNSTATE

A Tale of Two Gluon Distributions

[F. Dominguez, C. Marquet, BX and F. Yuan, 11]

I. Weizsäcker Williams gluon distribution

$$xG^{(1)} = \frac{S_\perp}{\pi^2\alpha_s}\frac{N_c^2-1}{N_c} \times \int \frac{d^2r_\perp}{(2\pi)^2}\frac{e^{-ik_\perp\cdot r_\perp}}{r_\perp^2}\left(1-e^{-\frac{r_\perp^2 Q_s^2}{2}}\right) \quad \Leftarrow$$

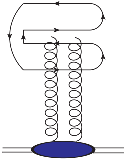

II. Color Dipole gluon distributions:

$$xG^{(2)} = \frac{S_\perp N_c}{2\pi^2\alpha_s} \times \int \frac{d^2r_\perp}{(2\pi)^2} e^{-ik_\perp\cdot r_\perp}\nabla^2_{r_\perp}N(r_\perp) \quad \Leftarrow$$

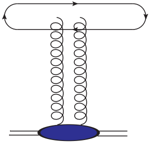

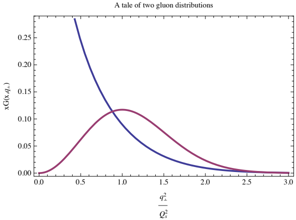

A Tale of Two Gluon Distributions

In terms of operators (known from TMD factorization), we find these two gluon distributions can be defined as follows: [F. Dominguez, C. Marquet, BX and F. Yuan, 11]

I. Weizsäcker Williams gluon distribution:

$$xG^{(1)} = 2\int \frac{d\xi^- d\xi_\perp}{(2\pi)^3 P^+} e^{ixP^+\xi^- - ik_\perp \cdot \xi_\perp} \mathrm{Tr}\langle P|F^{+i}(\xi^-,\xi_\perp)\mathcal{U}^{[+]\dagger}F^{+i}(0)\mathcal{U}^{[+]}|P\rangle.$$

II. Color Dipole gluon distributions:

$$xG^{(2)} = 2\int \frac{d\xi^- d\xi_\perp}{(2\pi)^3 P^+} e^{ixP^+\xi^- - ik_\perp \cdot \xi_\perp} \mathrm{Tr}\langle P|F^{+i}(\xi^-,\xi_\perp)\mathcal{U}^{[-]\dagger}F^{+i}(0)\mathcal{U}^{[+]}|P\rangle.$$

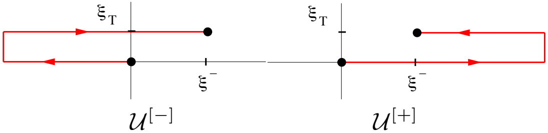

Remarks:

- The WW gluon distribution is the conventional gluon distributions. In light-cone gauge, it is the gluon density. (Only final state interactions.)
- The dipole gluon distribution has no such interpretation. (Initial and final state interactions.)
- Both definitions are gauge invariant.
- Same after integrating over $q_\perp$.

A Tale of Two Gluon Distributions

In terms of operators, we find these two gluon distributions can be defined as follows: [F. Dominguez, C. Marquet, BX and F. Yuan, 11]

I. Weizsäcker Williams gluon distribution:

$$xG^{(1)} = 2\int \frac{d\xi^- d\xi_\perp}{(2\pi)^3 P^+} e^{ixP^+\xi^- - ik_\perp\cdot\xi_\perp} \mathrm{Tr}\langle P|F^{+i}(\xi^-,\xi_\perp)\mathcal{U}^{[+]\dagger}F^{+i}(0)\mathcal{U}^{[+]}|P\rangle.$$

II. Color Dipole gluon distributions:

$$xG^{(2)} = 2\int \frac{d\xi^- d\xi_\perp}{(2\pi)^3 P^+} e^{ixP^+\xi^- - ik_\perp\cdot\xi_\perp} \mathrm{Tr}\langle P|F^{+i}(\xi^-,\xi_\perp)\mathcal{U}^{[-]\dagger}F^{+i}(0)\mathcal{U}^{[+]}|P\rangle.$$

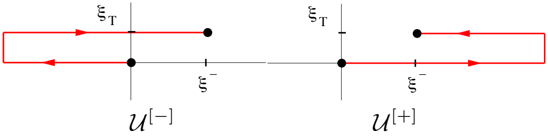

Questions:

- Can we distinguish these two gluon distributions? Yes, We Can.
- How to measure $xG^{(1)}$ directly? DIS dijet.
- How to measure $xG^{(2)}$ directly? Direct γ+Jet in pA collisions. For single-inclusive particle production in pA up to all order.
- What happens in gluon+jet production in pA collisions? It's complicated!

DIS dijet

[F. Dominguez, C. Marquet, BX and F. Yuan, 11]

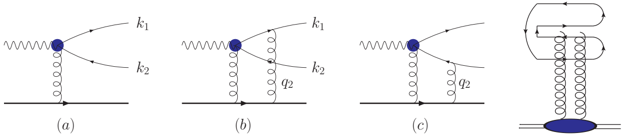

$$\frac{d\sigma^{\gamma_T^* A\to q\bar{q}+X}}{d\mathcal{P}.\mathcal{S}.} \propto N_c\alpha_{em}e_q^2\int\frac{\mathrm{d}^2x}{(2\pi)^2}\frac{\mathrm{d}^2x'}{(2\pi)^2}\frac{\mathrm{d}^2b}{(2\pi)^2}\frac{\mathrm{d}^2b'}{(2\pi)^2}e^{-ik_{1\perp}\cdot(x-x')}$$
$$\times e^{-ik_{2\perp}\cdot(b-b')}\sum\psi_T^*(x-b)\psi_T(x'-b')$$
$$\underbrace{\left[1+S_{x_g}^{(4)}(x,b;b',x')-S_{x_g}^{(2)}(x,b)-S_{x_g}^{(2)}(b',x')\right]}_{-u_iu_j'\frac{1}{N_c}\langle\mathrm{Tr}\left[\partial^i U(v)\right]U^\dagger(v')\left[\partial^j U(v')\right]U^\dagger(v)\rangle_{x_g}\Rightarrow\text{Operator Def}},$$

- Eikonal approximation $\Rightarrow$ Wilson Line approach [Kovner, Wiedemann, 01].
- In the dijet correlation limit, where $u=x-b\ll v=zx+(1-z)b$
- $S_{x_g}^{(4)}(x,b;b',x')=\frac{1}{N_c}\left\langle\mathrm{Tr}U(x)U^\dagger(x')U(b')U^\dagger(b)\right\rangle_{x_g}\neq S_{x_g}^{(2)}(x,b)S_{x_g}^{(2)}(b',x')$
- Quadrupoles are generically different objects and only appear in dijet processes.

DIS dijet

The dijet production in DIS.

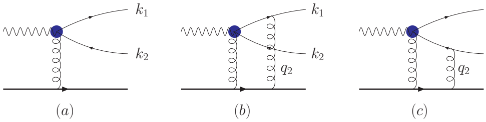

TMD factorization approach:

$$\frac{d\sigma^{\gamma_T^* A \to q\bar{q}+X}}{d\mathcal{P}.\mathcal{S}.} = \delta(x_{\gamma^*} - 1) x_g G^{(1)}(x_g, q_\perp) H_{\gamma_T^* g \to q\bar{q}},$$

Remarks:

- Dijet in DIS is the only physical process which can measure Weizsäcker Williams gluon distributions.
- Golden measurement for the Weizsäcker Williams gluon distributions of nuclei at small-x. The cross section is directly related to the WW gluon distribution.
- EIC and LHeC will provide us a perfect machine to study the strong gluon fields in nuclei. Important part in EIC and LHeC physics.

γ+Jet in pA collisions

The direct photon + jet production in pA collisions. (Drell-Yan follows the same factorization.)
TMD factorization approach:

$$\frac{d\sigma^{(pA\to\gamma q+X)}}{d\mathcal{P}.\mathcal{S}.} = \sum_f x_1 q(x_1,\mu^2) x_g G^{(2)}(x_g, q_\perp) H_{qg\to\gamma q}.$$

Remarks:

- Independent CGC calculation gives the identical result in the correlation limit.
- Direct measurement of the Color Dipole gluon distribution.

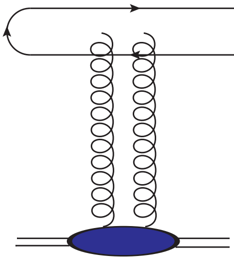

DY correlations in pA collisions

[Stasto, BX, Zaslavsky, 12]

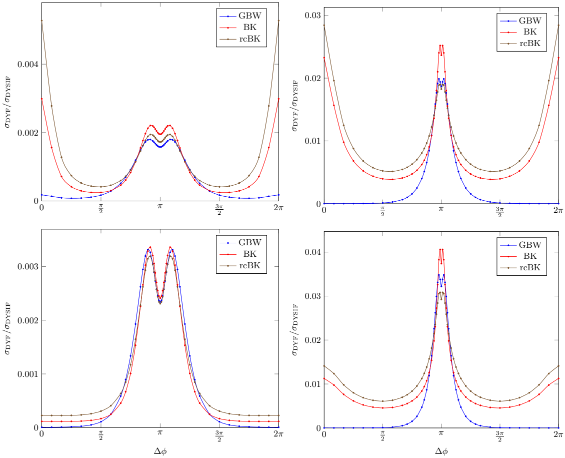

$M = 0.5, 4\text{GeV}, Y = 2.5$ at RHIC dAu. $M = 4, 8\text{GeV}, Y = 4$ at LHC pPb.

- Partonic cross section vanishes at $\pi \Rightarrow$ Dip at π.
- Prompt photon calculation [J. Jalilian-Marian, A. Rezaeian, 12]

PENNSTATE 1855

STAR measurement on di-hadron correlation in *dA* collisions

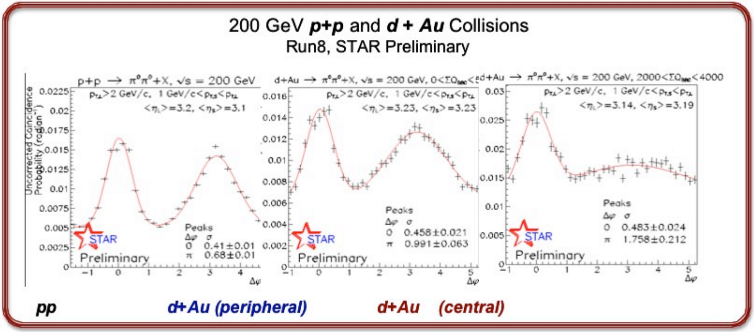

- There is no sign of suppression in the $p + p$ and $d + Au$ peripheral data.
- The suppression and broadening of the away side jet in $d + Au$ central collisions is due to the multiple interactions between partons and dense nuclear matter (CGC).
- Probably the best evidence for saturation.

First calculations on dijet production

Quark+Gluon channel [Marquet, 07] and [Albacete, Marquet, 10]

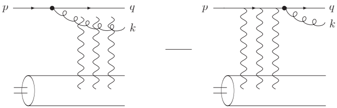

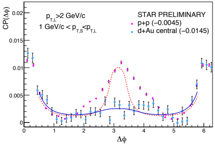

- Prediction of saturation physics.
- All the framework is correct, but over-simplified 4-point function.
- Improvement [F. Dominguez, C. Marquet, BX and F. Yuan, 11.]

$$S_{x_g}^{(4)}(x_1,x_2;x_2',x_1') \simeq e^{-\frac{C_F}{2}[\Gamma(x_1-x_2)+\Gamma(x_2'-x_1')]}$$
$$-\frac{F(x_1,x_2;x_2',x_1')}{F(x_1,x_2';x_2,x_1')}\left(e^{-\frac{C_F}{2}[\Gamma(x_1-x_2)+\Gamma(x_2'-x_1')]}-e^{-\frac{C_F}{2}[\Gamma(x_1-x_1')+\Gamma(x_2'-x_2)]}\right)$$

Dijet processes in the large N_c limit

The Fierz identity:

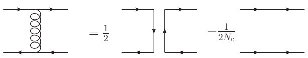

and

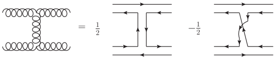

Graphical representation of dijet processes

$g \to q\bar{q}$:

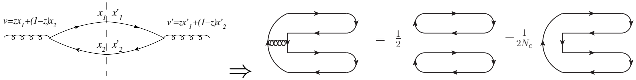

$q \to qg$

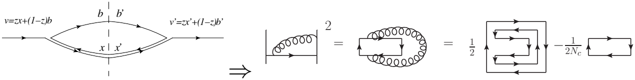

$g \to gg$

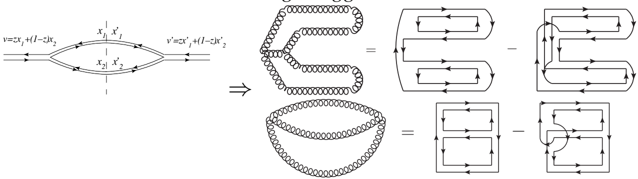

PENNSTATE

The Octupole and the Sextupole are suppressed.

Gluon+quark jets correlation

Including all the $qg \to qg$, $gg \to gg$ and $gg \to q\bar{q}$ channels, a lengthy calculation gives

$$\begin{aligned}\frac{d\sigma^{(pA\to\text{Dijet}+X)}}{d\mathcal{P}.\mathcal{S}.} &= \sum_q x_1 q(x_1,\mu^2)\frac{\alpha_s^2}{\hat{s}^2}\left[\mathcal{F}_{qg}^{(1)}H_{qg}^{(1)}+\mathcal{F}_{qg}^{(2)}H_{qg}^{(2)}\right] \\ &+x_1 g(x_1,\mu^2)\frac{\alpha_s^2}{\hat{s}^2}\left[\mathcal{F}_{gg}^{(1)}\left(H_{gg\to q\bar{q}}^{(1)}+\frac{1}{2}H_{gg\to gg}^{(1)}\right)\right. \\ &\left.+\mathcal{F}_{gg}^{(2)}\left(H_{gg\to q\bar{q}}^{(2)}+\frac{1}{2}H_{gg\to gg}^{(2)}\right)+\mathcal{F}_{gg}^{(3)}\frac{1}{2}H_{gg\to gg}^{(3)}\right],\end{aligned}$$

with the various gluon distributions defined as

$$\begin{aligned}\mathcal{F}_{qg}^{(1)} &= xG^{(2)}(x,q_\perp),\quad \mathcal{F}_{qg}^{(2)}=\int xG^{(1)}\otimes F\,, \\ \mathcal{F}_{gg}^{(1)} &= \int xG^{(2)}\otimes F,\quad \mathcal{F}_{gg}^{(2)}=-\int\frac{q_{1\perp}\cdot q_{2\perp}}{q_{1\perp}^2}xG^{(2)}\otimes F\,, \\ \mathcal{F}_{gg}^{(3)} &= \int xG^{(1)}(q_1)\otimes F\otimes F\,,\end{aligned}$$

where $F=\int\frac{d^2r_\perp}{(2\pi)^2}e^{-iq_\perp\cdot r_\perp}\frac{1}{N_c}\left\langle \text{Tr}U(r_\perp)U^\dagger(0)\right\rangle_{x_g}$.

Remarks:

- Only the term in NavyBlue color was known before.
- This describes the dihadron correlation data measured at RHIC in forward dAu collisions.

PENNSTATE 1855

Illustration of gluon distributions

The various gluon distributions:

$$xG^{(1)}_{\rm WW}(x,q_\perp),\quad \mathcal{F}^{(1)}_{qg}=xG^{(2)}(x,q_\perp),$$

$$\mathcal{F}^{(1)}_{gg} = \int xG^{(2)}\otimes F,\quad \mathcal{F}^{(2)}_{gg}=-\int\frac{q_{1\perp}\cdot q_{2\perp}}{q^2_{1\perp}}xG^{(2)}\otimes F\,,$$

$$\mathcal{F}^{(3)}_{gg} = \int xG^{(1)}(q_1)\otimes F\otimes F\,,\quad \mathcal{F}^{(2)}_{qg}=\int xG^{(1)}\otimes F$$

6 different gluon distributions

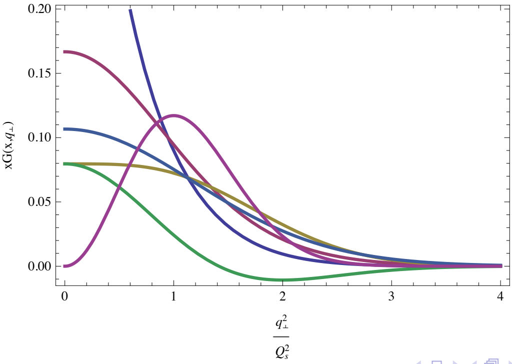

Comparing to STAR and PHENIX data

Physics predicted by C. Marquet. Further calculated in[A. Stasto, BX, F. Yuan, 11]

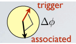

For away side peak in both peripheral and central *dAu* collisions

$$C(\Delta\phi) = \frac{\int_{|p_{1\perp}|,|p_{2\perp}|} \frac{d\sigma^{pA\to h_1 h_2}}{dy_1 dy_2 d^2p_{1\perp} d^2p_{2\perp}}}{\int_{|p_{1\perp}|} \frac{d\sigma^{pA\to h_1}}{dy_1 d^2p_{1\perp}}}$$

$$J_{dA} = \frac{1}{\langle N_{\rm coll}\rangle} \frac{\sigma_{dA}^{\rm pair}/\sigma_{dA}}{\sigma_{pp}^{\rm pair}/\sigma_{pp}}$$

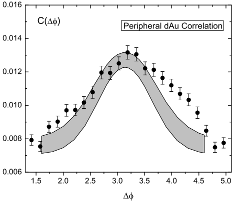

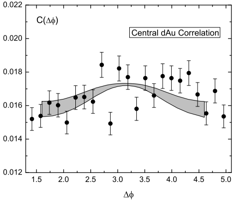

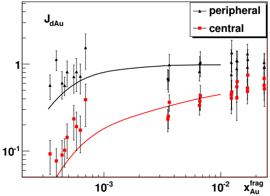

- Using: $Q_{sA}^2 = c(b)A^{1/3}Q_s^2(x)$.
- Physical picture: Dense gluonic matter suppresses the away side peak.

Conclusion and Outlook

Conclusion:

- DIS dijet provides direct information of the WW gluon distributions. Perfect for testing CGC, and ideal measurement for EIC and LHeC.
- Modified Universality for Gluon Distributions:

	Inclusive	Single Inc	DIS dijet	γ +jet	g+jet
$xG^{(1)}$	$\times$	$\times$	$\surd$	$\times$	$\surd$
$xG^{(2)}$, F	$\surd$	$\surd$	$\times$	$\surd$	$\surd$

$\times \Rightarrow$ Do Not Appear. $\surd \Rightarrow$ Apppear.

- Two fundamental gluon distributions. Other gluon distributions are just different combinations and convolutions of these two.
- The small-x evolution of the WW gluon distribution, a different equation from Balitsky-Kovchegov equation;[Dominguez, Mueller, Munier, Xiao, 11]
- Dihadron correlation calculation agrees with the RHIC STAR and PHENIX data.

PENNSTATE

Outlook

[Dominguez, Marquet, Stasto, BX, in preparation] Use Fierz identity:

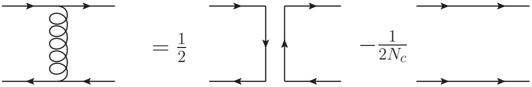

- The three-jet (same rapidity) production processes in the large N_c limit:

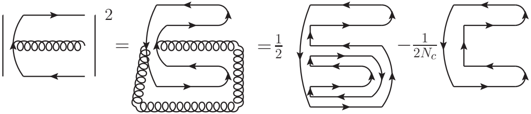

$q\bar{q}g$-jet

- In the large N_c limit at small-x, the dipole and quadrupole amplitudes are the only two fundamental objects in the cross section of multiple-jet production processes at any order in terms α_s.
- Other higher point functions, such as sextupoles, octupoles, decapoles and duodecapoles, etc. are suppressed by factors of $\frac{1}{N_c^2}$.

PENNSTATE